Orientational Isomers and Monolayer Structure of CH_3D Physisorbed on NaCl(100)

Kent A. Davis and George E. Ewing*

Department of Chemistry, Indiana University, Bloomington, Indiana 47405

Received: September 3, 1998; In Final Form: January 13, 1999

Polarized infrared spectra of CH_3D adsorbed on NaCl(100) in the temperature range 5−37 K are reported. Analysis of the ν_2 spectral region reveals one transition dipole perpendicular to the surface and two oriented at $70 \pm 20°$ (or $110 \pm 20°$) from the surface normal. These features are assigned to C−D stretching vibrations of molecules oriented in a tripod conformation with the deuterium in the "top" position (D-up) and in a tripod with the deuterium in a "base" position (D-down). The fraction of D-up orientational isomers is shown to decrease with decreasing temperature. An energy splitting of 100 ± 20 J mol^{-1} between D-up and D-down orientational isomers is consistent with this temperature dependence. A phase transition near 30 K associated with changes in rotatory motions has been observed. Below this transition, a splitting in the D-down region is shown to be statistically consistent with the position of the deuterium atoms on the surface. Some point toward substrate chloride ions and others point toward 'gaps' between chloride ions.

I. Introduction

Solid-phase and matrix-isolated CH_4 and its isotopomers display a range of intriguing phenomena. Much attention has been paid to the rotational levels and orientational ordering behavior of these systems. The three phases of the solid methanes differ chiefly in the extent of rotational freedom with molecules in phase I behaving like free rotors, while phases II and III contain sublattices with molecules that vary from nearly free rotation to libration and tunneling motions.[1,2] Theoretical models[3,4] based upon the octupole−octupole interactions between methane molecules have successfully described the structure of the two highest temperature phases of the solid methanes (for CH_4, the only phases accessible without pressure elevation) while the exact structure of the third, lowest temperature phase remains elusive.[1,5,6]

Although studies of methane in two-dimensional physisorbed phases have been somewhat less common, a number of groups have characterized methane monolayers and submonolayers on insulator or graphite surfaces using a variety of experimental and theoretical techniques.

A prime motivating factor in the study of these systems is examination of the possibility of phase transitions and free or nearly free rotation of adsorbed methane paralleling changes observed in the three-dimensional solid methanes. Neutron scattering studies of methane adsorbed on graphite[7−9] have shown an array of tunneling levels as has similar work using an MgO substrate.[10] A Monte Carlo study of methane adsorbed on graphite revealed two phases differentiated by their rotational order about a 3-fold axis perpendicular to the surface.[11] A molecular field model, analogous to the classic James−Keenan model of solid methane,[3] was also used to explore the phase transitions of a methane adlayer on graphite.[12] A molecular dynamics study of CD_4 adsorbed on MgO showed a coordinated "cogwheeling" motion of the entire adlayer.[13,14]

Another goal of most of this research has been to determine the conformation of adsorbed methane molecules and the structure of the extended adlayer. Various studies have preferred a tripod conformation (three hydrogens nearest to the surface) or a dipod conformation (two hydrogens nearest to the surface) for physisorbed methane. It has been proposed that, in general, methane will physisorb in a tripod conformation when the methane−substrate interactions dominate methane-methane interactions, while a dipod conformation is favored in the opposite case.[15,16] Current data suggest that methane dipods are favored on an MgO(100) substrate[17,18] while tripod methane is preferred on the basal plane of graphite.[8,12] Polarized Fourier transform infrared (FTIR) spectroscopic studies of CH_4 physisorbed on NaCl(100) support a symmetric adsorption conformation (i.e., tripod or dipod) but no conclusive preference for either.[19−21] On the basis of theoretical arguments, these studies have placed CH_4 on top of Na^+ sites. Helium atom scattering (HAS) experiments have been useful in determining the unit mesh structure.[21] Above 30 K a 1×1 unit cell was identified while below this temperature a 2×2 structure was favored. However, HAS is insensitive to hydrogen position and, consequently, to adsorbate conformation. Using polarized FTIR, we have shown that CHD_3 adsorbed on NaCl(100) exists in a tripod conformation.[22] In addition to conformation determination, a type of orientational ordering was observed. Two types of tripod orientational isomers were distinguished, those with the single hydrogen atom in the tripod "top" position (H-up) and those with the hydrogen in one of the three tripod "base" positions (H-down). The H-up isomer was shown to be stable at low temperatures with an energy separation of 7 ± 2 cm^{-1} between the two isomers. A similar distinction between orientational isomers has been observed for CH_3D adsorbed on graphite.[23,24] In those studies, inelastic neutron scattering and heat capacity data were used to reproduce the librational ground-state energy levels which revealed a 3 cm^{-1} gap between D-up and D-down tunneling levels (with the D-down isomer stable for this molecule).

The current work concerns CH_3D adsorbed on NaCl(100). Several questions remain that we wish to address here. Does the observation of a tripod conformation of CHD_3 mean that other methane isotopomers also adsorb as tripods? Can observation of the orientational isomers of CH_3D tell us anything new

* To whom correspondence should be addressed.

10.1021/jp983620j CCC: $18.00
Published on Web 02/24/1999

about the origin of the energy difference between isomers or about the orientational ordering mechanism? Is there evidence for quasi free rotation or cogwheeling? The present work attempts to satisfy some of these questions.

II. Experiment

Adsorption experiments are performed on the (100) faces of a pair of cleaved sodium chloride single crystals. Fresh surfaces are obtained by cleavage of single crystal blocks of NaCl (Harshaw/Bicron) in a dry nitrogen atmosphere using a hammer and chisel. Freshly cleaved crystals are attached to a sample mount and inserted into an ultrahigh vacuum (UHV) chamber. The copper sample mount, described elsewhere,[25] holds two 25 $\times$ 25 $\times$ 3 mm crystal slabs with the surfaces to be interrogated at an angle of 120° from each other. The center of the sample holder is hollowed out to allow for the transmission of infrared light through both crystals. The sample mount containing the crystals is bolted onto a copper cryostat work surface. Temperatures between 40 and 5 K were attained by transfer of helium from a liquid helium reservoir to the copper cryostat. Temperature stability of $\pm$0.4 K was maintained by regulating the helium flow rate and was monitored by a rhodium−iron thermistor and a temperature controller (Lakeshore Cryotronics). Thermal contact with the cold work surface was enhanced by placing small pieces of indium foil between the crystals and the sample mount and between the sample mount and the cryostat work surface. Since the temperature sensor measures the temperature *in* the helium flow and not the temperature of the NaCl surface, H_2 condensation experiments were performed to determine the minimum achievable temperature. The minimum surface temperature of 5.2 K was determined by comparing the pressure of H_2 needed to form the solid on the NaCl crystals with the known vapor pressure of hydrogen. Pressures were measured using an ion gauge and UHV conditions (base pressure 1×10^{-9} mbar) were maintained using an ion pump (Varian). A leak valve served to allow inlet of low pressures of gas into the vacuum chamber.

A Fourier transform infrared spectrometer (Bruker IFS-66) was used to collect infrared spectra of the adsorbed molecules. A focused beam of infrared radiation from a globar source was transmitted through the UHV entrance window, through the pair of NaCl crystals (propagation vector 60° from surface normal), and out the UHV exit window. The entire beam path was isolated from the atmosphere and purged with dry nitrogen gas. The polarization of the infrared light to be analyzed was selected using a wire grid polarizer (International Crystal Labs), and the beam is then focused onto the element of an indium−antimonide (InSb) detector.

To begin an experiment, the crystal temperature was lowered from the storage temperature of 400 K to 30 K. After collecting background interferograms using both E_p (electric field parallel with the plane of incidence) and E_s (electric field perpendicular to the plane of incidence) polarized light, methane was admitted to the chamber and sample interferograms were obtained. In general, 1000 scans (about 10 min) were averaged for both background and sample data. Spectra were obtained by Fourier transform using four-point apodization and two times zero-filling. The interferograms were transformed at 0.5 and 2 cm^{-1}. Sample and background spectra were ratioed to obtain the absorbance.

Although at 30 K monolayer growth can occur at 3×10^{-9} mbar, surface contamination (mainly carbon monoxide emitted from the stainless steel vacuum chamber walls) could be more easily avoided by forming the monolayer more rapidly at a pressure of 2×10^{-8} mbar. As this pressure is quite near the vapor pressure (3×10^{-8} mbar) of the neat solid, extreme care was required to inhibit multilayer growth from commencing as the monolayer was cooled. In practice, this is achieved by warming the crystals a few degrees while the leak valve for gas admission was closed and the gaseous methane pumped away. The monolayer was then warmed or cooled to the desired temperature. Monolayers formed in this way behaved identically to those formed more slowly at lower pressures and were stable for hours.

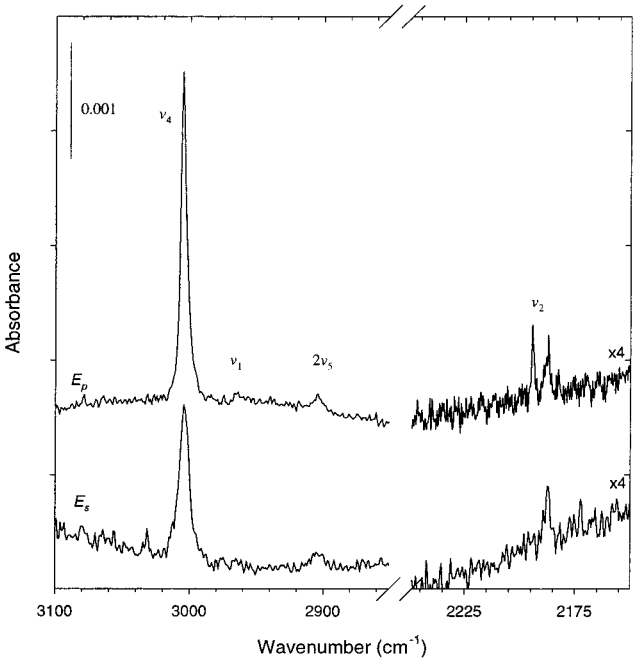

Figure 1. E_p and E_s spectra of the ν_2 and ν_4 vibrational modes and the $\nu_1-2\nu_5$ Fermi resonance pair for monolayer CH_3D on NaCl(100) at 33 K. The spectra have been scaled by a factor of 4 in the ν_2 region.

III. Results

Since the frequencies of the CH_3D vibrational modes are not significantly shifted following physisorption, we can make band assignments based upon gas-phase transition frequencies.[26−29] The CH_3D molecule belongs to the C_{3v} point group and has nine normal modes of vibration: three totally symmetric (a_1) vibrations and three doubly degenerate (e) vibrations. All the vibrations are infrared active, but since the InSb detector is only sensitive to frequencies above 1800 cm^{-1}, we are only able to observe the stretching regions ν_1 (a_1 symmetric C−H stretch), ν_2 (a_1 symmetric C−D stretch), ν_4 (e asymmetric C−H stretch), and an overtone of ν_5 (e asymmetric C−D bend). The vibrational frequencies, $\tilde{\nu}$, and bandwidths, Γ, (measured at half-absorbance) were obtained by fitting the spectra using Gaussian profiles. Figure 1 shows the E_p and E_s spectra of physisorbed CH_3D at 33 K. The E_p spectra, in the frequency range of the C−H stretching vibration, contain features centered at 2905, 2975, and 3006 cm^{-1} and corresponding bandwidths 12, 12, and 8 cm^{-1}. The highest frequency band is assigned to the ν_4 (e) vibration. Its E_s component appears at frequency 3004 cm^{-1} with bandwidth 10 cm^{-1}. The slight frequency shift between these spectra and the broadness of the feature suggests that it obscures an overlapping *pair* of bands with different polarization dependencies. We shall return to this suggestion later. The other two features in this region can be assigned to ν_1 (a_1) and the first overtone of ν_5 ($a_1 + a_2 + e$). The overtone is observed as a consequence of Fermi resonance of its a_1 component, with ν_1

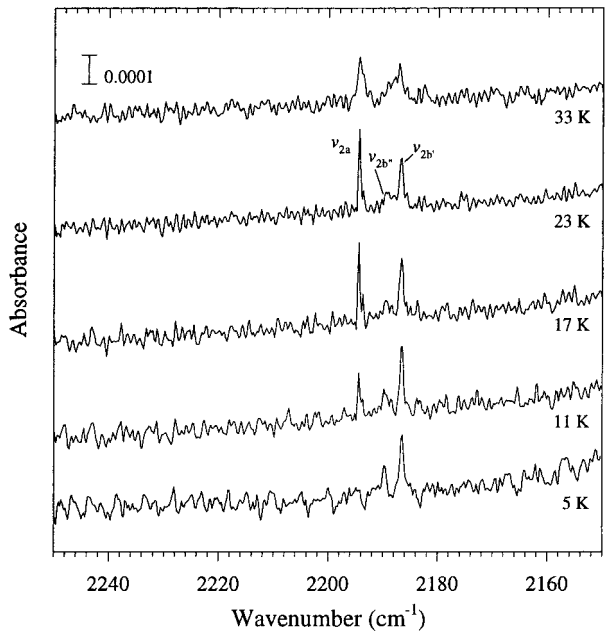

Figure 2. E_p spectra of the ν_2 C−D stretching vibration at several temperatures.

producing two bands that are admixtures of ν_1 and $2\nu_5$.[26−28] In the gas phase, the two bands have roughly equal intensities, whereas in the absence of the resonance phenomenon, the intensity of the overtone would be negligible. If there are subtle differences in the frequency and bandwidth of these features in the two polarizations as we observed for ν_4, we cannot detect them because of their low absorbance. In the region of ν_2 (a_1) we observe what appear to be two spectral features. The higher frequency band, ν_{2a}, at 2194.4 cm^{-1} is narrow with a bandwidth of less than 0.5 cm^{-1} (the limit of our resolution) and is observed in the E_p spectrum only. The second band, ν_{2b}, is centered at 2186 cm^{-1} and is much broader, with a bandwidth of 2 cm^{-1}. This feature is present in spectra of both polarizations.

As the temperature is lowered, the ν_1, ν_4, and $2\nu_5$ bands undergo no apparent change. In the ν_2 region, however, a discontinuous change occurs in bandwidths where ν_{2a} at 2 cm^{-1} in the temperature region 37−33 K drops to less than 0.5 cm^{-1} at 23 K and below. This discontinuity, suggesting a phase change, appears near 30 K. In addition, the ν_{2b} feature narrows with an accompanying splitting into $\nu_{2b'}$ at 2186 cm^{-1} and $\nu_{2b''}$ at 2189 cm^{-1}. These changes at 33 K and below, are shown in Figure 2 for spectra of E_p polarization. At 23 K, $\nu_{2b'}$ has a bandwidth of 0.8 cm^{-1} and $\nu_{2b''}$ is slightly broader with a bandwidth of 1.5 cm^{-1}. While $\nu_{2b''}$ has less than one-quarter of the absorbance of $\nu_{2b''}$, because of the larger bandwidth, the integrated absorbance of $\nu_{2b''}$ is one-half of the integrated absorbance of $\nu_{2b''}$. As the temperature is lowered from 17 K, it becomes clear that the absorbance of ν_{2a} decreases while that of ν_{2b} ($\nu_{2b'} + \nu_{2b''}$) increases. This behavior continues as the temperature is lowered until at 5 K the ν_{2a} feature has essentially vanished, leaving only the $\nu_{2b'}$ and $\nu_{2b''}$ features. These changes in $\nu_{2b'}$ and $\nu_{2b''}$ are mirrored in the corresponding E_s spectra. All temperature-dependent changes are fully reversible.

That Figures 1 and 2 contain spectra of a *full* monolayer is clear based on several observations. Formation of the adlayer at slightly higher pressure leads to multilayer formation, as evidenced by the appearance of the broad single features for each vibrational mode that are anticipated for three-dimensional CH_3D. Thus, we are at the highest coverage possible without solid formation. The absence in our spectra of the broad feature characteristic of the solid (especially noticeable in the ν_2 region where all bands are quite sharp) is evidence that multilayers are not formed. In addition, the intensity of a contribution from possible multilayers in excess of the first would be likely to change from one experiment to the next in opposition to our observations.

IV. Discussion

Our focus in this discussion will be to determine the orientation of adsorbed CH_3D molecules and the structure of the monolayer. We shall attempt to integrate this new data with what is already known about other methane isotopomers on NaCl(100). We first review methods for obtaining orientational information from polarization data. We then discuss the origin of the ν_2 splittings and use the experimentally determined transition dipole orientations to establish the adsorbate conformation. Next, we will examine the temperature dependence of the orientational isomers within the observed conformation. Finally, we examine interactions between CH_3D molecules and the substrate and between neighboring CH_3D molecules and we propose a monolayer structure consistent with our observations.

A. Photometry and Transition Dipole Orientation Expressions. Photometry relations derived from Beer's law can be used to determine the transition dipole orientations for each of the infrared absorptions of methane on NaCl(100). These relations have been described in detail elsewhere,[22,30,31] so here we present only the relation for the integrated absorbance, $\tilde{A}_p$, used for E_p polarized light, which will be modified in the discussion to follow.

$$\tilde{A}_p = \frac{NS\bar{\sigma}_g}{2.303\cos\theta}\left[\frac{3\cos^2\alpha\sin^2\theta}{(1+\alpha_e U_\perp^\circ)^2} + \frac{3}{2}\frac{\sin^2\alpha\cos^2\theta}{(1+\alpha_e U_\parallel^\circ)^2}\right] \quad (1)$$

In this equation, N is the number of surfaces available for adsorption ($N = 4$ in our experiments), S is the surface density of Na^+Cl^- pairs ($S = 6.4 \times 10^{14}$ molecules/cm^2), and $\bar{\sigma}_g$ is the integrated absorption cross section of the adsorbate. Here, as elsewhere,[19−21] the adsorbed CH_4 molecules are taken to be over Na^+ sites, so S may be read as the molecular density of the monolayer. The trigonometric terms in θ account of the tilt of the NaCl(100) surfaces (and the adsorbed monolayer) with respect to the interrogating light. For our surfaces $\theta = 60°$. The laboratory fixed Z axis is defined to be perpendicular to the (100) surface and the X and Y axes are in the surface plane. The angle, α, refers to the tilt of the adsorbate transition dipole away from the Z axis. Another expression relating the response of adsorbate transition dipoles to E_s polarized light yields the $\tilde{A}_s$ integrated absorbance. We shall not use this expression directly, and it is discussed elsewhere.[22,30,31]

The expressions for $\tilde{A}_p$ and $\tilde{A}_s$ also include terms to account for induced dipoles. This has been derived by others[19,32,33] in terms of the molecular polarizability, $\alpha_e = 259$ pm,[34] and $U_\parallel^\circ$ or $U_\perp^\circ$, which contain sums over all induced dipoles in the layer. These are given by $U_\perp^\circ = -2U_\parallel^\circ = S_3 a^{-3}$ where $S_3 = 9.03$ is an Ewald sum that has been evaluated analytically[35] and $a = 398$ pm is the surface lattice spacing for NaCl(100) and the proposed distance between nearest-neighbor methane molecules. This distance has been shown to differ from the bulk lattice spacing by only 0.5%.[36]

The photometry relations for $\tilde{A}_p$ and $\tilde{A}_s$ have been solved for the transition dipole tilt angle to obtain[22,30]

$$\alpha = \tan^{-1}\left[\left(\frac{6(1+\alpha_e U_{||}^{\circ})^2/(1+\alpha_e U_{\perp}^{\circ})^2}{8(\tilde{A}_p/\tilde{A}_s)/(1+\eta^2)-1}\right)^{1/2}\right] \qquad (2)$$

where $\eta = 1.52$, the index of refraction of NaCl, was carried over from the $\tilde{A}_s$ relationship. Since α from $\tilde{A}_p$ (and $\tilde{A}_s$) appears only as $\sin^2\alpha$ or $\cos^2\alpha$ in eq 1, its determination from eq 2 is ambiguous. Thus, the value α is indistinguishable from $\pi - \alpha$. As we shall see this ambiguity does not affect our ability here in determining molecular orientation.

B. Splittings and Adsorbate Conformation. Before attempting to use the spectra to determine the conformation of the adsorbed CH_3D molecules, we shall explore the possible origins of the ν_2 splittings. While there are three spectral bands in this region, we can simplify matters by first treating $\nu_{2b'}$ and $\nu_{2b''}$ together as ν_{2b}. The identical temperature and polarization dependencies of these bands suggests that the same mechanism causes the splitting between ν_{2a} and both bands within ν_{2b}.

The splitting between ν_{2a} and ν_{2b} is 8.4 cm^{-1} at 33 K. Several splitting mechanisms have been considered previously for CHD_3 adsorbed on NaCl(100),[22] and the arguments are the same for CH_3D so we will not recount them in detail here. Briefly, we can discount degeneracy breaking since this mode is nondegenerate. Coupling between oscillators within the unit mesh can be eliminated due to the small magnitude of the C−D stretch transition moment. The possibility of adsorption in two or more different adsorption sites (which very likely would have different adsorption energies) can be excluded since we observe all bands growing in tandem as the monolayer is formed. The most reasonable remaining alternative is that the molecules are adsorbed in identical adsorption sites but they are oriented differently.

For any particular conformation of CH_3D molecules (e.g., dipod or tripod) there are up to four permutations of the three hydrogen atoms and the deuterium. These different structures formed by permuting the hydrogen and deuterium atoms we call orientational isomers. In general, the transition dipoles of these orientational isomers have different tilt angles. As a result of these unique orientations and the slightly different environments of the transition dipoles, each orientational isomer is expected to absorb at a slightly different frequency and can be spectroscopically distinguished. For CHD_3 adsorbed on NaCl(100), a tripod conformation was established based upon determination of the orientations of the transition dipoles of its two orientational isomers.[22]

For a CH_3D tripod, we also expect two types of orientational isomers, one with the deuterium in the tripod "top" position (D-up) and one with the deuterium in one of the three "base" positions (D-down). Figure 3 shows the tripod orientational isomers. The transition dipole of the ν_2 vibration is directed along the C−D bond; hence, the D-up transition dipole is positioned along the surface normal ($\alpha_2 = 0°$) while the D-down transition dipole is oriented at the tetrahedral angle of $\alpha_2 = 109.5°$ (or 70.5°) from the surface normal.

In the other most likely conformation, a CH_3D dipod would also have two types of orientational isomers, D-up and D-down. While the transition dipole for both of these isomers has the same tilt angle of $\alpha_2 = 55.5°$, it might be reasoned that a splitting could still occur due to the different environments (e.g., electric field) experienced by a C−D group vibrating against the surface and a C−D group oscillating into the vacuum.

We now make use of the polarization absorbance measurements in Figure 1 at 33 K together with eq 2 to determine the transition dipole orientation and from this the molecular orientation. For ν_{2a}, absorbance is significant for E_p but not apparent for E_s. If we imagine a feeble absorbance in E_s, it must be less than the noise level. We must then have from the spectra in Figure 1 the ratio $\tilde{A}_p/\tilde{A}_s > 5$ This is consistent with a transition dipole tilt angle of $0° < \alpha_{2a} < 20°$. For $\nu_{2b'}$ we find $\tilde{A}_p/\tilde{A}_s = 0.7 \pm 0.3$, which corresponds to a tilt angle of $\alpha_{2b'} = 70 \pm 20°$ (or $110 \pm 20°$). Similarly, for $\nu_{2b''}$ we find $\alpha_{2b''} = 70 \pm 20°$ (or $110 \pm 20°$). For the bands in the C−H stretching region, the slight frequency shift between the E_s and E_p features and their broadness suggests a concealed splitting of similar origin to that of the ν_2 mode. A similar splitting of the C−D stretching mode was observed for CHD_3.[22] Since the 33 K spectra contain ν_2 features with their transition dipoles oriented at $0° < \alpha_{2a} < 20°$and $\alpha_{2b} = 70 \pm 20°$ (or $110 \pm 20°$), our data clearly support the tripod conformation and exclude the dipod structure.

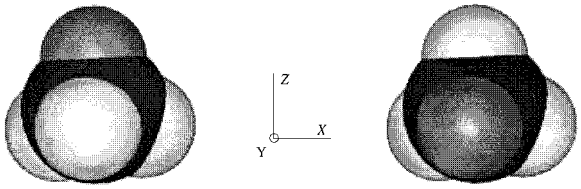

Figure 3. The D-up and D-down orientational isomers of the tripod conformation of CH_3D. The deuteriums are gray and the hydrogens look white. The position of the deuterium in the D-down orientation isomer can be changed by permutation with either of its two base hydrogen atoms.

Thus far in the conformation assignment, we have entirely neglected one conformation. The monopod (or inverted tripod) has transition dipole orientations that are indistinguishable from the tripod. This dismissal seems warranted, however, based on earlier calculations and physical intuition based upon the nature and magnitude of dispersion and electrostatic attractions for the two conformations.

We have successfully used the splitting between ν_{2a} and ν_{2b} to assign CH_3D on NaCl(100) to a tripod conformation. We have not yet explained the splitting between the $\nu_{2b'}$ and $\nu_{2b''}$ features. This task we will postpone until after a discussion of the temperature dependence of the orientational isomers.

C. Temperature Dependence of Orientational Isomers. *1. Zero-Point Orientational Isomer Levels.* Here, we explore the temperature-dependent absorbance changes in the ν_2 region as revealed in Figure 2. We we will concentrate our attention on the disappearance of the ν_{2a} band, which we have just associated with a D-up tripod orientational isomer of CH_3D, although the analysis detailed here is applicable, with slight modification, to the bands due to the D-down orientational isomer.

In their presented form, the photometry equation, eq 1, is temperature independent. The disappearance of the band corresponding to the D-up orientational isomer demonstrates that the surface density of D-up (and D-down) adsorbates is changing with temperature. We will modify the density of adsorbates, S, to include a Boltzmann temperature dependence.

The system we are discussing contains two energy levels which correspond to the D-up and D-down orientational isomers. Since there are three equivalent D-down isomers, one level is triply degenerate. The fraction of D-up orientational isomers is given by[37]

$$f_u = \frac{e^{-hc\epsilon/kT}}{3 + e^{-hc\epsilon/kT}} \qquad (3)$$

where ϵ is the spacing between the D-down and D-up energy levels and the D-down level is taken as the zero of energy. The surface density of D-up molecules is given by $S_u = f_u S$, where as before $S = 6.4 \times 10^{14}$ molecules/cm^2 is the total monolayer

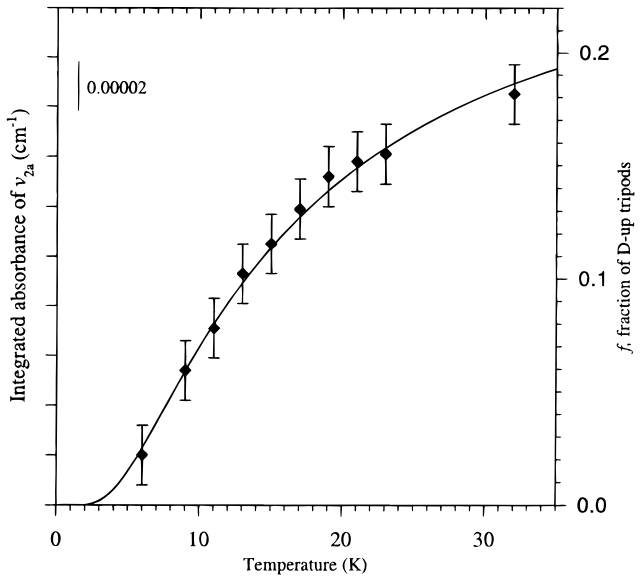

Figure 4. Temperature dependence of the D-up tripod orientational isomer of CH_3D adsorbed on NaCl(100). Symbols represent experimental data, and the curve shows the results of the two energy level model with level separation $\epsilon = 9$ cm^{-1}.

density. After substitution of this revised surface density into eq 1, we can use the observed temperature dependence to calculate the energy gap, ϵ, between the two orientational isomer energy levels. We fit the ν_{2a} integrated absorbance, using eq 1, our modified surface density function, S_u, and the D-up tripod transition dipole orientation of $\alpha_{2a} = 0°$. We have two undetermined parameters that are adjusted, ϵ and the integrated cross section, $\bar{\sigma}_g$.

The results of this procedure are shown in Figure 4. The energy difference value between D-up and D-down orientational isomers consistent with the ν_{2a} integrated absorbance is $\epsilon = 9 \pm 2$ cm^{-1} (110 ± 20 J mol^{-1}). This result is in reasonable accord with the 7 ± 2 cm^{-1} (80 ± 20 J mol^{-1}) value established for CHD_3 adsorbed on NaCl(100). A consistency is also found with neutron scattering experiments on monolayer CH_3D physisorbed on graphite that reveal a 3 cm^{-1} splitting between D-down and D-up states.[23,24]

2. Orientational Isomer Conversion. Orientational isomer energy levels observed for CHD_3 adsorbed on NaCl(100) and conversion between them to achieve low-temperature ordering was shown to be consistent with a tunneling mechanism. A tunneling calculation was made using the eigenfunctions of a restricted rotor Hamiltonian.[38,39] The calculated tunnel splitting was very small as expected due to the high (400 cm^{-1}) barrier that was assumed for rotation about one of the tripod "base" C−D bonds, and the calculated tunneling time (10^{-8} s) was considerably shorter than required for conversion on an experimentally relevant time scale.

While for our purposes it is pointless to attempt a more quantitatively precise calculation of the tunneling frequency for conversion between orientational isomers, this treatment is, of course, flawed in not accounting for the asymmetry of the potential wells due to the splitting of the orientational isomers of CH_3D (as well as CHD_3). Inclusion of the asymmetry requires the additional consideration of conservation of energy. A transition from a D-up tripod to a D-down tripod requires not only barrier penetration but a 9 cm^{-1} relaxation. Such a transition would have a rate given by Fermi's Golden Rule:[40]

$$w = \frac{2\pi}{\hbar}|\langle D_{up}|V|D_{down}\rangle|^2 \rho(E) \quad (4)$$

in which the bracketed term is the overlap of the wave functions of the D-up and D-down states and $\rho(E)$ is the density of states in the D-down potential well.

We know that the overlap is small as we are able to observe the D-up and D-down orientational isomers rather than the mixture expected if the levels combined considerably. A reasonable guess is that the overlap integral is of similar order of magnitude to that previously calculated using a symmetric sinusoidal potential.

The tunneling rate is scaled by the density of states to account for the efficiency of energy transfer as a molecule relaxes from the D-up energy level to the D-down level. The density of states in the region 9 cm^{-1} above the D-down ground state is unknown, but we can consider some of the states involved. While the preponderance of the bulk phonon modes of NaCl are higher in energy, a few of the $3N$ modes associated with N substrate ions within a domain will be in this low-energy region. Those phonons primarily associated with surface oscillations tend to have frequencies that are lower than the frequencies of the bulk. These frequencies are also altered by the presence of an adlayer.[41]

In addition to the substrate modes, there exist phonon modes of the adsorbate layer itself that are perhaps even more likely to couple with the tunneling motion. In one reasonable tunneling pathway, a tripod "base" hydrogen rotates through the tetrahedral angle to the tripod "top" position (displacing a deuterium which ends up in a "base" position opposite the hydrogen starting point). This pathway, assuming the remaining hydrogens are not forced to tunnel along the NaCl surface, has the additional effect of moving the molecule along the surface, away from the original Na^+ site effectively coupling to the adsorbate frustrated translational mode.

A nearly free rotation of methane about an axis normal to the surface has been proposed but not experimentally verified. The D-up to D-down relaxation could readily be accomplished by coupling with this rotation since the separation of the lower rotational levels of a CH_3D free rotor would be on the order of 5−10 cm^{-1}.[27] We see, however, no spectroscopic evidence for such rotations.

3. Upper Vibrational State ($\nu_2 = 1$) Orientational Isomer Levels. Armed with knowledge of the size of the energy gap between the vibrational ground state ($\nu_2 = 0$) of the D-up and D-down orientational isomers and the vibrational frequencies of these isomers, we are able to determine the energy splitting between orientational isomer levels in the vibrationally excited state ($\nu_2 = 1$). The D-down isomer has been shown to be associated with the lower energy in the vibrational ground state with the D-up level 9 cm^{-1} higher, but because of our incomplete understanding of the origin of the energy gap, we have difficulty determining which of the orientational isomer levels will be more stable in the $\nu_2 = 1$ level. One scheme is depicted in Figure 5. Assuming that there is no orientational isomer conversion coupled with vibrational excitation, the only level configuration possible for the upper vibrational state is a lower energy D-down level separated from the higher D-up level by 16 cm^{-1}.

A comparison of the current experiment with the results for CHD_3[22] and CH_2D_2[42] adsorbed on NaCl(100) leads us to what seems be a developing pattern. The lowest energy orientational isomer in all three cases is the one with the most deuteriums down (nearest the substrate). It has been shown that zero-point energy is a major influence in determining the conformation of

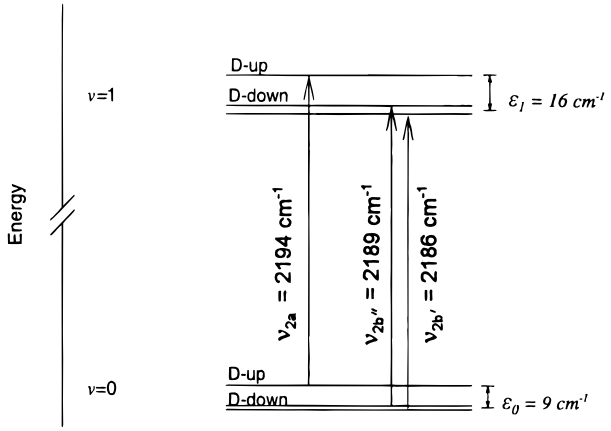

Figure 5. Energy level diagram for the transition from $\nu_2 = 0$ to $\nu_2 = 1$.

methane adsorbed on graphite and germanium[16] and it is reasonable to suspect that zero-point energy plays a similar role in determining the stability of orientational isomers. A physical picture, albeit a simplistic one, is that since the amplitude of the zero-point C−H stretching vibration is larger than the zero-point C−D stretch amplitude, it is reasonable to suspect that the isomer with the most deuteriums down would be most stable since the molecules can pack closer to the surface when more of the larger amplitude C−H oscillations are directed away from the surface and/or neighboring molecules.

It would seem, based on energy considerations related solely to the effect of vibrational displacements on molecular packing, that excitation into the C−D group would make the D-down orientation less stable. Since this is contrary to the energy level scheme we favor in Figure 5, we must then suppose that the stew of repulsion, dispersion, dipole and multipole interactions associated with the $\nu_2 = 1$ level continue to favor D-down as the most stable orientation.

D. Monolayer Structure. Thus far, we have discussed the molecular conformation and the temperature dependence of the populations of the orientational isomers of the tripod conformation. What remains to be explored is the origin of the ν_{2b} splitting into its $\nu_{2b'}$ and $\nu_{2b''}$ components. The main point to consider in choosing among various proposed splitting mechanisms is that the two components appear to have identical polarization and temperature dependencies. In effect, both of these factors demonstrate that both ν_{2b} features arise from the C−D stretching vibrations of D-down orientational isomers. Since both of the ν_{2b} features arise from transition dipoles with identical tilt angles, we can directly compare the integrated absorbance of the two bands to get an estimate of the relative populations. At 5 K, the ratio is $\tilde{A}_{2b'}/\tilde{A}_{2b''} \approx 2$. At higher temperatures, $\nu_{2b''}$ broadens more than $\nu_{2b'}$ but the integrated absorbance ratio remains roughly 2:1. Therefore we say that the $\nu_{2b'}$ band represents about twice as many molecules as does $\nu_{2b''}$ across the range of temperatures studied. We can exclude oscillator coupling[43] and multiple adsorption sites[44−46] as the origin of the splitting by the same arguments used for explaining the splitting between ν_{2a} and ν_{2b}. That the features are not due to rotational excitation, of either a three-dimensional free rotor or a planar free rotor, is clear given that there should be several more rotational lines (spaced by 3−5 cm^{-1}, depending upon the orientational isomer in question) at all but the lowest temperatures. We are left with the interpretation of $\nu_{2b'}$ and $\nu_{2b''}$ as arising from vibrations of D-down tripods in two distinct *positions* on the NaCl(100) surface.

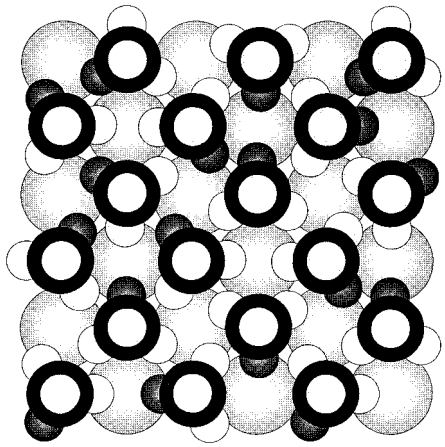

Figure 6. Proposed 5 K monolayer structure of CH_3D adsorbed on NaCl(100). CH_3D molecules are shown adsorbed over sodium sites with hydrogens (white spheres) and deuteriums (dark gray spheres) distributed randomly among the three tripod "base" positions.

One possible monolayer structure for CH_3D is shown in Figure 6. A similar monolayer model has been previously proposed for CH_4 on NaCl(100)[19] and CD_4 on MgO(100).[14] Since only D-down CH_3D orientational isomers are shown, this structure is appropriate for discussion of the low-temperature ($\leq$5 K) monolayer. Each CH_3D molecule has been positioned with surface plane projection of one of the tripod "base" C−H (or C−D) bonds pointing toward a neighboring chloride ion (along the rows and columns of Figure 6) and the projections of the other two bonds directed 30° away from the centers of two other neighboring chloride ions (more or less along the diagonals of Figure 6). We will use the labels C−D → Cl and C−D → gap to refer to C−D bonds with their surface projections pointing toward Cl^- ions or toward the "gap" between Cl^- ions, respectively. This arrangement was the result of a calculation of the minimization of the Coulomb repulsion of three hydrogens, represented by partially negative point charges, and the four nearest chloride ions as a tripod CH_3D molecule directly over Na^+ was rotated about the surface normal. This model is simplistic in that dispersion interactions and higher order electric multipoles have not been considered and there is even some disagreement about the direction of the C−H bond dipoles of methane,[47,48] but little damage will be sustained to the overall line of argument if a slightly different structure is assumed since the result that there are twice as many C−D → gap positions as C−D → Cl positions seems to arise naturally as a result of placing a molecule with a 3-fold axis on a substrate with 4-fold symmetry. This monolayer structure is nicely in accord with the observed 2:1 absorbance ratio of the ν_{2b} features.

The proposed structure was arrived at by considering soley the effect of packing differences of CH_3D against the substrate. A second possible origin of the ν_2 splitting we shall explore is the influence of neighboring CH_3D molecules. Assuming that the molecules are positioned on top of Na^+ sites 398 pm apart and have a van der Waals radius of 191 pm,[48] then the boundaries of neighboring molecules are separated by 16 pm. If we include the extension produced by oscillating bonds and librational motion, it is reasonable that the C−D vibration could be affected by the proximity and type (hydrogen or deuterium) of a neighboring atom. For the molecules with C−D bonds directed toward Cl^- ions, the deuterium has two nearest-neighbor atoms. These are on different methane molecules and therefore the C−D stretching vibration could be perturbed by either a pair of hydrogen atoms (HH), a pair of deuterium atoms

(DD), or the combination of deuterium and hydrogen atoms (HD). For the case of a C−D bond directed away from Cl^-, there are also two nearest-neighbor atoms (one of them is actually slightly nearer than the other). These neighboring atoms are also attached to different methane molecules, so the same combinations of hydrogen and deuterium atoms occur here. Since the D-up and D-down molecules interconvert as the temperature is changed, the neighboring atom combinations will change as well. Assuming a random distribution of deuterium atoms in any of the tripod "base" positions and using eq 1 for the fraction of D-down molecules, we can calculate for each case the probability that the neighboring atoms are deuterium or hydrogen or both. There are a few different ways that we could use the calculated probabilities. If, as a first attempt, we separate molecules with a nearby deuterium from those whose neighbors only present hydrogen atoms, we find the ratio, (HD + DD)/HH, to be 1.25 at 0 K and 0.78 at high temperature. On the other hand, if we separate the H-down molecules into a type that has two deuterium neighbors and another type whose neighbors have either two hydrogen atoms or a hydrogen and a deuterium, we find a ratio, (HH + HD)/DD of 8 at 0 K and 4.2 at high temperature. Since neither of these cases approaches the observed 2:1 absorbance ratio of $\nu_{2b'}$ and $\nu_{2b''}$, we conclude that intermolecular interactions cannot account of the appearance of this doublet.

We have seen that the splitting of the ν_2 vibration of the D-down orientational isomers of CH_3D is more compatible with a model involving perturbations caused by the neighboring substrate Cl^- ions than one incorporating interactions with nearest-neighbor methane molecules. This finding loosely parallels a recently used potential for methane on NaCl(100) where the largest part of the crystalline field resulted from methane−substrate rather than methane−methane interactions.[15] One might question why this effect was not observed for CHD_3 adsorbed on NaCl(100). The only band for which we might have expected to see this effect was the ν_1 C−H stretching mode. The spectral band corresponding to the H-down orientational isomer of CHD_3 was rather broad at high temperatures, and because for CHD_3 the H-down isomer is higher energy, the band was not observable at low temperatures where the bandwidth may have been smaller. Therefore, even though this splitting may occur for CHD_3, it is would be impossible to observe due to the low number of H-down adsorbates at low temperature.

Returning to Figure 5, we can estimate the energy difference between the C−D → gap and C−D → Cl positions of the D-down orientation isomer of CH_3D on NaCl(100). The 3 cm^{-1} difference of $\nu_{2b'}$ and $\nu_{2b''}$ is interpreted to arise because of the difference in splittings in the $\nu_2 = 1$ and $\nu_2 = 0$ levels. If, as in the case of the D-up and D-down orientational energy, we take the positional energy difference to be considerably greater in the $\nu_2 = 1$ level than in the $\nu_2 = 0$ level, we can imagine the spacing between C−D → gap and C−D → Cl levels in the ground vibrational state to be say 1−2 cm^{-1}. The corresponding temperature of ∼2 K would explain why we see no variation in the abundances of the C−D → gap and C−D → Cl positions even at temperatures as low as 5.2 K.

E. Phases of Methanes on NaCl(100). We turn our attention now to the phases of physisorbed methane. The three solid phases are well-known, but analogous two-dimensional phases, while predicted, are elusive experimentally. Evidence of CH_4 adlayer rotatory motion on crystallites of NaCl at 100 K has been reported.[49] A phase transition between a 1 × 1 and 2 × 2 unit cell, suggested to accompany a change from two-dimensional quasifree rotor layer and a hindered librator layer, has been suggested by helium atom scattering data for CH_4 adsorbed on NaCl(100) at a temperature near 30 K. Our spectral data for CH_3D on NaCl(100) show a quite dramatic change in the ν_2 region near 30 K. The ratio of the polarized absorbances shows that no conformation change is involved. For CH_3D molecules perturbed by their position with respect to the substrate, rotational motion would tend to average the influence of the substrate and effectively eliminate any discrimination between C−D → Cl or C−D → gap molecules. The disappearance of $\nu_{2b'}$ and $\nu_{2b''}$ splitting above 30 K is consistent with this interpretation. The identification by HAS of a phase transition in CH_4 on NaCl(100) above 30 K, which is associated with a change in rotatory motion, is likely related to the phase transition we observe for the CH_3D isotope.

Evidence of concerted rotation of a layer of adsorbates, cogwheeling, was not found in our spectroscopic measurements for any methane isotopes on single-crystal NaCl(100).

We have observed for both tripod CH_3D and CHD_3 on NaCl(100) another type of phase. Orientationally ordered phases have been identified near 5 K for CHD_3 and for CH_3D where, in both cases, the deuterium atoms are against the surface. The ordered structure of CHD_3 is, in fact, a ferroelectric phase since all of the molecules have their vibrationally induced dipoles[50] aligned.

At even lower temperatures (probably well below 2 K), an additional ordering could take place in which all the CH_3D molecules on NaCl(100) are in the C−D → gap position. But the ordering need not stop here. The weak vibrationally induced dipole of the CH_3D molecules (along the C_3 axis) could cause the alignment of dipoles along one diagonal of the NaCl(100) face to be paired with respect to the dipoles along neighboring diagonals. We anticipate this ordered phase to appear at a temperature of less than 1 K.

It is clear that the phases of two-dimensional methane crystals are numerous and intricate, and we have yet to consider the role of nuclear spin.

V. Conclusion

We have uncovered three levels of structural detail for CH_3D on NaCl(100). The first level concerns the conformation. Our spectroscopy finds that the molecules are arranged as tripods against the NaCl(100) surface. The second level of detail reveals that essentially all tripods are oriented with the D-atom against the surface for temperatures below 10 K. Finally, in this orientation, we are able to distinguish two positions of the D-atom with respect to the Cl^- ions of the (100) face. Above a phase transition near 30 K, these two positions become indistinct.

Evidence for free rotations, or cogwheeling motions, has eluded our spectroscopic observations.

Acknowledgment. We thank the National Science Foundation for their support through Grant NSF CHE-9505892.

References and Notes

(1) Maki, K.; Kataoka, Y.; Yamamoto, T. *J. Chem. Phys.* **1979**, *70*, 655.
(2) Morrison, J. A. *J. Chem. Thermodyn.* **1988**, *20*, 641.
(3) James, H. M.; Keenan, T. A. *J. Chem. Phys.* **1959**, *31*, 12.
(4) Yamamoto, T.; Kataoka, Y.; Okada, K. J. *J. Chem. Phys.* **1977**, *66*, 2701.
(5) Maki, K.; Kataoka, Y.; Yamamoto, T. *Acta Crystallogr. A* **1975**, *31*, S188.
(6) O'Shea, S. F. *J. Chem. Phys.* **1978**, *68*, 5435.

(7) Newbery, N. W.; Rayment, T.; Smalley, M. V.; Thomas, R. K.; White, J. W. *Chem. Phys. Lett.* **1978**, *59*, 461.
(8) Smalley, M. V.; Hüller, A.; Thomas, R. K.; White, J. W. *Mol. Phys.* **1981**, *44*, 533.
(9) Inaba, A.; Ikeda, S.; Skarbek, J.; Thomas, R. K.; Carlile, C. J.; Sivia, D. S. *Phys. B* **1995**, *213*/*214*, 643.
(10) Larese, J. Z.; Hastings, J. M.; Passell, L.; Smith, D.; Richter, D. *J. Chem. Phys.* **1991**, *95*, 6997.
(11) Maki, K.; Nosé, S. *J. Chem. Phys.* **1979**, *71*, 1392.
(12) O'Shea, S. F.; Klein, M. L. *J. Chem. Phys.* **1979**, *71*, 2399.
(13) Alavi, A. *Phys. Rev. Lett.* **1990**, *64*, 2289.
(14) Alavi, A. *Mol. Phys.* **1990**, *71*, 1173.
(15) Smith, D. *Chem. Phys. Lett.* **1994**, *228*, 379.
(16) Bruch, L. W. *J. Chem. Phys.* **1987**, *87*, 5518.
(17) Coulomb, J. P.; Madih, K.; Croset, B.; Lauter, H. J. *Phys. Rev. Lett.* **1985**, *54*, 1536.
(18) Jung, D. R.; Cui, J.; Frankl, D. R. *Phys. Rev. B* **1991**, *43*, 10042.
(19) Quattrocci, L. M.; Ewing, G. E. *J. Chem. Phys.* **1992**, *96*, 4205.
(20) Quattrocci, L. M.; Ewing, G. E. *Chem. Phys. Lett.* **1992**, *197*, 308.
(21) Heidberg, J.; Schönekäs, O.; Weiss, H.; Lange, G.; Toennies, J. P. *Ber. Bunsen-Ges. Phys. Chem.* **1995**, *99*, 1370.
(22) Davis, K. A.; Ewing, G. E. *J. Chem. Phys.* **1997**, *107*, 8073.
(23) Inaba, A.; Skarbek, J.; Lu, J. R.; Thomas, R. K.; Carlile, C. J.; Sivia, D. S. *J. Chem. Phys.* **1995**, *103*, 1627.
(24) Ball, P. C.; Inaba, A.; Morrison, J. A.; Smalley, M. V.; Thomas, R. K. *J. Chem. Phys.* **1990**, *92*, 1372.
(25) Chang, H.-C.; Richardson, H. H.; Ewing, G. E. *J. Chem. Phys.* **1988**, *89*, 7561.
(26) Ginsburg, N.; Barker, E. F. *J. Chem. Phys.* **1935**, *3*, 668.
(27) Wilmshurst, J. K.; Bernstein, H. J. *Can. J. Chem.* **1957**, *35*, 226.
(28) Richardson, E. H.; Brodersen, S.; Krause, L.; Welsh, H. L. *J. Mol. Spectrosc.* **1962**, *8*, 400.
(29) Shimanouchi, T. *Tables of Molecular Vibrational Frequencies*; National Bureau of Standards: Washington, DC, 1972; Vol. 1.
(30) Berg, O.; Ewing, G. E. *Surf. Sci.* **1989**, *220*, 207.
(31) Richardson, H. H.; Chang, H.-C.; Noda, C.; Ewing, G. E. *Surf. Sci.* **1989**, *216*, 93.
(32) Chabal, Y. J. *Surf. Sci. Rep.* **1988**, *8*, 211.
(33) Chen, W.; Schaich, W. L. *Surf. Sci.* **1989**, *218*, 580.
(34) Gislason, E. A.; Bundenholzer, F. E.; Jorgensen, A. D. *Chem. Phys.* **1977**, *47*, 434.
(35) Van der Hoff, B. M. E.; Benson, G. C. *Can. J. Phys.* **1953**, *31*, 1087.
(36) Benedek, G.; Brusdeylins, G.; Doak, R. B.; Skofronick, J. G.; Toennies, J. P. *Phys. Rev. B* **1983**, *28*, 2104.
(37) Hill, T. *An Introduction to Statistical Thermodynamics*; Addison-Wesley: Reading, MA, 1960.
(38) Eyring, H.; Walter, J.; Kimball, G. E. *Quantum Chemistry*; Wiley: New York, 1944.
(39) Herschbach, D. R. *J. Chem. Phys.* **1959**, *31*, 91.
(40) Merzbacher, E. *Quantum Mechanics*; Wiley: New York, 1970.
(41) Brusdeylins, G.; Doak, R. B.; Toennies, J. P. *Phys. Rev. B* **1983**, *27*, 3662.
(42) Davis, K. A.; Ewing, G. E. Unpublished results.
(43) Heidberg, J.; Kampshoff, E.; Kühnemuth, R.; Schönekäs, O.; Stein, H.; Weiss, H. *Surf. Sci. Lett.* **1990**, *226*, L43.
(44) Dai, D.; Ewing, G. E. *J. Chem. Phys.* **1994**, *100*, 8432.
(45) Dai, D. *J. Chem. Phys.* **1996**, *104*, 2461.
(46) Dai, D. *J. Chem. Phys.* **1996**, *104*, 6338.
(47) Stone, A. J. *Intermolecular Forces*; Oxford: New York, 1995.
(48) Hirschfelder, J.; Curtiss, C.; Bird, R. *Molecular Theory of Gases and Liquids*; Wiley: New York, 1964.
(49) Edling, J. A.; Richardson, H. H.; Ewing, G. E. *J. Mol. Struct.* **1987**, *157*, 167.
(50) Hollenstein, H.; Marquardt, R. R.; Quack, M.; Suhm, M. A. *J. Chem. Phys.* **1994**, *101*, 3588.